Proceedings of CONF-MCEE 2026 Symposium: Advances in Sustainable Aviation and Aerospace Vehicle Automation
DOI: 10.54254/2755-2721/2026.KA27726

Thermo-Responsive Photonic Hydrogel for Smart Window Applications

William Wu

St. George's School, Vancouver, Canada
williamwujh527@gmail.com

Abstract. In this study, we report a versatile strategy for the fabrication of large-area, structurally colored photonic crystal films and their thermo-responsive hydrogel composites using monodisperse silica nanoparticles. Silica nanoparticles with controlled sizes (100–390 nm) were synthesized via the Stöber method and characterized by transmission electron microscope and dynamic light scattering, confirming excellent monodispersity and size uniformity. These nanoparticles were self-assembled into highly ordered 3D photonic crystal structures using a vertical deposition method, producing vivid structural colors tunable across the visible spectrum in accordance with Bragg's law. To overcome mechanical fragility, the photonic crystals were embedded within a hydrogel scaffold, yielding free-standing, large-area films that preserved structural order while providing thermo-responsive color shifts. Upon heating, the films exhibited reversible blue-shifts due to hydrogel contraction, as confirmed by in situ UV–vis spectroscopy, demonstrating robust and repeatable optical responsiveness. The photonic hydrogel are planned to be further explored for potential applications, including temperature indicators and radiative cooling materials, leveraging both optical feedback and passive thermal management. The combination of tunable structural color, mechanical stability, and dynamic response establishes these photonic hydrogels as a promising platform for functional coatings, smart windows, and energy-efficient optical devices.

Keywords: photonic crystal films, structural color, hydrogel, silica nanoparticles

1. Introduction

The increasing global demand for air conditioning has raised both energy consumption and greenhouse gas emissions, posing a significant environmental challenge. Today, approximately 2 billion air conditioning units are in operation worldwide, with projections suggesting this number could reach 5.5 billion by 2050. In 2022, space cooling alone consumed roughly 2,100 terawatt-hours (TWh) of electricity, accounting for nearly 7% of global electricity use and 20% of building electricity demand [1]. This escalating energy consumption highlights the need for passive and adaptive thermal management strategies, particularly those capable of reducing reliance on energy-intensive air conditioning [2]. One promising approach is passive daytime radiative cooling, which reflects incident sunlight ($\lambda \approx 0.3–2.5$ μm) while emitting thermal radiation through the atmospheric transparency window ($\lambda \approx 8–13$ μm) to dissipate heat into space [3,4]. Existing radiative cooling

© 2026 The Authors. This is an open access article distributed under the terms of the Creative Commons Attribution License 4.0 (https://creativecommons.org/licenses/by/4.0/).

DOI: 10.54254/2755-2721/2026.KA27726

solutions, including metamaterials and nanoporous polymer films, operate continuously regardless of environmental temperature, sometimes accelerating heat loss and increasing energy demands for heating [5,6]. Therefore, there is significant interest in designing adaptive systems capable of responding dynamically to environmental temperature.

In this context, we propose a smart window system that combines structurally colored photonic crystals (PCs) with thermo-responsive hydrogels, enabling simultaneous visual appeal, temperature indication, and energy modulation. Photonic crystals, composed of periodic arrangements of dielectric materials with contrasting refractive indices, can manipulate light by forming photonic bandgaps (PBGs) that selectively reflect specific wavelengths [7]. PCs can be engineered as 1D, 2D, or 3D structures Figure 1, providing highly tunable and customizable optical properties for applications in optical switching, sensing, and display technologies [8-11]. Hydrogels are cross-linked polymer networks capable of absorbing and retaining large amounts of water [12]. Thermo-responsive hydrogels, such as polyacrylamide, undergo reversible volume changes in response to temperature, swelling below their lower critical solution temperature (LCST) and contracting above it [13-17]. When integrated with PCs, hydrogels allow dynamic tuning of lattice spacing, producing reversible shifts in reflected wavelength (e.g., blue-shifts upon heating). This behavior enables the system to act as a temperature indicator, where the visible color changes in response to ambient temperature, providing a clear and intuitive visual cue without additional electronics. Simultaneously, this system can be designed for radiative cooling applications while maintaining aesthetic appeal. The hydrogel matrix and silica nanoparticles allow high infrared emission and selective reflection, enabling the window to passively shed heat when exposed to sunlight [18-21].

Recent advances in dynamic structural coloration have been demonstrated in multilayer films, metasurfaces, and photonic crystals, achieving high-resolution control of visible colors even below the diffraction limit [22]. By combining this optical control with stimuli-responsive hydrogels, the present work provides a platform for large-area, mechanically robust, and tunable photonic crystal composites. These materials can simultaneously deliver visual cues, aesthetic appeal, and energy regulation, offering a promising approach for adaptive smart windows that integrate temperature indication, decorative functions, and radiative cooling capabilities.

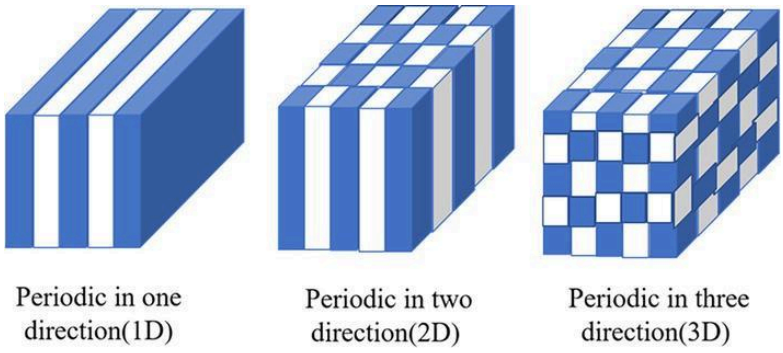

Figure 1. Schematic representation of 1D, 2D, and 3D photonic crystal structures[11]

2. Experimental section

2.1. Chemicals

The chemicals used in this study are listed in the following table. Unless stated explicitly, all chemicals were used without further purification (Table 1).

DOI: 10.54254/2755-2721/2026.KA27726

Table 1. List of chemicals used in this study

Chemical name	Specifications	Supplier
Tetraethyl orthosilicate (TEOS)	98%	Aladdin Scientific Corp.
Ammonium hydroxide	25%-28%	Macklin Inc.
Ethanol	99.5%	Macklin Inc.
Deionized water	N/A	Millipore Milli Q
Acrylamide (AAm)	99.0%	Aladdin Scientific Corp.
Acrylic Acid (AA)	>99%	Aladdin Scientific Corp.
N,N'-Methylenebis(acrylamide) (BIS)	99%	Aladdin Scientific Corp.
Sulfobetaine Methacrylate (SBMA)	98%	Aladdin Scientific Corp.
Irgacure 2959	98%	Aladdin Scientific Corp.

2.2. Instruments

The instruments used in this study are listed in the following table. The sample preparation method for each instrument will be described later in the section of characterizations (Table 2).

Table 2. List of instruments and equipment used in this study

Instrument name	Model	Manufacturer
Magnetic stirrer	FK-1	Shandong Fangke
Drying oven	AX30	Verder Scientific
Transmission Electron Microscope (TEM)	FEI Tecnai G2 F20	Thermo Fisher Scientific
Dynamic Light Scattering (DLS)	Malvern Zetasizer Nano ZS90	Malvern Panalytical
Scanning Electron Microscope (SEM)	ZEISS Sigma 300	Carl Zeiss
UV-Vis spectrometer	UV3600	Shimadzu Corp.
In-situ temperature-dependent UV spectrometer	3600-Plus	Shimadzu Corp.

2.3. Characterizations

TEM observations were carried out in FEI Tecnai G2 F20 microscope at an acceleration voltage of 200 kV. TEM samples were prepared by dropping the nanoparticle suspension (5 μL) onto carbon-coated copper grids and drying the sample at room temperature. SEM was performed using a ZEISS Sigma 300, operated at 3 kV and a working distance of 4–5 mm. The samples were prepared by adding the nanoparticle suspensions on a silicon wafer. After drying, they are mounted on aluminum stubs using conductive carbon tape and coated with Pt (10 nm) using a sputter coater. DLS was performed with a glass cuvette with round aperture on a ZETASIZER NANO-ZS90 with 633 nm He-Ne LASER (Malvern Panalytical). The nanoparticle suspensions (1 mL) were added to the cuvette and equilibrated for 5 min at room temperature (30 °C) before the measurements. Measurement angle, position, and attenuator were fixed at 173°, 6.0 mm, and 11, respectively.

DOI: 10.54254/2755-2721/2026.KA27726

2.4. Preparation of samples

2.4.1. Preparation of silica particles with different diameters

Silica microspheres were prepared using the Stöber method. As shown in Figure 2, a mixed solution of ammonia, water, and anhydrous ethanol was placed in bottle A, and a mixture of tetraethyl orthosilicate (TEOS) and anhydrous ethanol was placed in bottle B. Both solutions were preheated on a magnetic stirrer to the desired reaction temperature, then combined and transferred into a three-neck round-bottom flask equipped with a thermostatic heating magnetic stirrer. After stirring for 5 min, the reaction mixture gradually changed from colorless to milky white, and the reaction was completed after 2 h. The resulting suspension was centrifuged, and the supernatant was discarded. Anhydrous ethanol was then added to the precipitate, and any residual product adhering to the vessel walls was redispersed using an ultrasonic cleaner. The mixture was centrifuged again to remove unreacted starting materials, yielding the desired silica nanoparticles.

To obtain different sizes of silica nanoparticles, specific reaction conditions were used as below:

(1) Condition 1: At t = 2 h, T = 30 °C, [TEOS] = 0.2 mol, and [H_2O] = 10 mol, silica nanoparticles with diameters of approximately 100, 150, and 200 nm were obtained by adjusting the ammonia concentration to 0.5, 1.1, and 2.1 mol, respectively.

(2) Condition 2: At t = 2 h, T = 30 °C, [NH_3] = 1 mol, and [H_2O] = 10 mol, silica nanoparticles with diameters of approximately 250, 300, and 350 nm were obtained by adjusting the TEOS concentration to 0.2, 0.3, and 0.4 mol, respectively.

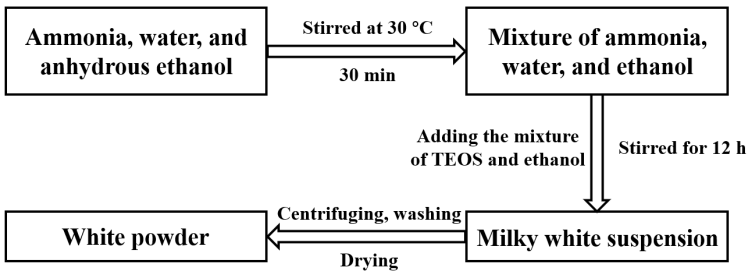

Figure 2. Flow chart of the process of preparation of silica particles with different sizes

2.4.2. Preparation of photonic crystal structural color films

Three-dimensional (3D) photonic crystal structural colors were fabricated from silica nanoparticle dispersions via a self-assembly method. Among various techniques, the vertical deposition self-assembly method was chosen for its simplicity, low equipment cost, controllable photonic crystal thickness, and relatively short fabrication time. This method is particularly advantageous for producing small-size, high-quality photonic crystals.

Glass slides were first cleaned by ultrasonic treatment in deionized ater and ethanol for 2 min each to remove surface impurities, then dried for later use. Monodisperse SiO2 microspheres (6–8 wt%) were ultrasonicated for 1 h prior to use. As shown in Figure 3, the dispersion was poured into a cylindrical glass vial, into which the cleaned glass slides were vertically inserted. Finally, the vial was placed in a thermostatic incubator at 60 °C for approximately 60 h to allow vertical deposition, resulting in the self-assembled photonic crystal structural color films.

DOI: 10.54254/2755-2721/2026.KA27726

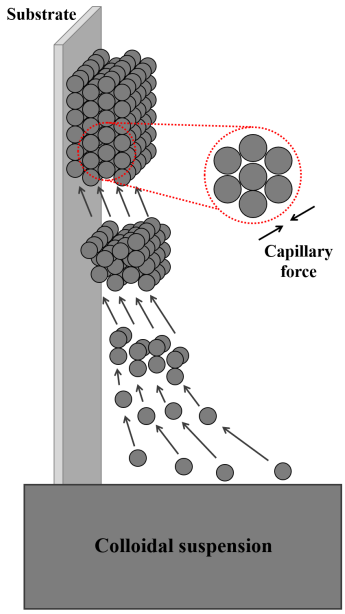

Figure 3. Schematic illustration of the photonic crystal film preparation via vertical deposition self-assembly method

2.4.3. Preparation of photoniccrystal hydrogels

The hydrogel precursor was prepared as follows: Acrylamide (AAm), acrylic acid (AA), N,N′-methylenebisacrylamide (BIS), sulfobetaine methacrylate (SBMA), the photoinitiator 2-hydroxy-4′-(2-hydroxyethoxy)-2-methylpropiophenone (Irgacure 2959), and deionized water were used as raw materials. A mixture containing 200 mmol AAm, 10 mmol SBMA, 10 mmol AA, 0.2 mmol BIS, and 16 g deionized water was placed in a beaker and stirred until a homogeneous solution was obtained. Subsequently, 1 mmol of photoinitiator Irgacure 2959 was added, and the mixture was stirred for 30 s.

The resulting hydrogel precursor solution was then transferred onto the previously fabricated photonic crystal structural color array. Polymerization was carried out under low-temperature conditions and UV irradiation to obtain the photonic crystal temperature-sensitive sensor. After polymerization, the temperature-sensitive hydrogel was obtained by manually peeling and transferring the product.

3. Results and discussions

Based on the experimental design, the results are organized into four sections: (1) preparation of silica nanoparticles, (2) self-assembly of silica nanoparticles, (3) structural color of photonic crystals, and (4) fabrication and thermo-responsive behavior of hydrogel-photonic crystal composite. Finally, we discuss the potential application of the hydrogel-photonic crystal composite in radiative cooling, outlining the next steps for this research.

3.1. Preparation of silica nanoparticles

To achieve structural color, this study employs three-dimensional (3D) photonic crystals as the primary strategy, as they typically produce highly bright, vivid, and saturated colors. These materials

DOI: 10.54254/2755-2721/2026.KA27726

derive their color not from pigments or dyes, but from periodic variations in refractive index that selectively reflect certain wavelengths of light via Bragg diffraction. A common approach to fabricate 3D photonic crystals is through the self-assembly of monodisperse nanoparticles into an ordered lattice. The degree of ordering in the nanoparticle arrangement directly determines the optical quality of the structural color: perfectly ordered crystals generate sharp and intense colors, whereas disordered structures lead to matte, dull, or washed-out appearances.

One of the most critical factors affecting crystal formation is particle size uniformity, often quantified by the polydispersity index (PDI). A lower polydispersity means that the nanoparticles have nearly identical sizes, which promotes close packing and minimizes lattice defects. In contrast, broader size distributions disrupt the periodic structure, preventing the formation of long-range order and thereby degrading the color intensity.

To obtain silica nanoparticles with the lowest possible polydispersity, we used the Stöber method, a well-established synthesis route known for producing highly monodisperse, spherical silica particles. The method relies on the controlled hydrolysis and condensation of a silicon alkoxide precursor, typically tetraethyl orthosilicate (TEOS), in an alcohol–water mixture under basic catalysis. In this study, ammonia served as the catalyst, while ethanol acted both as the solvent and as a medium to control reaction kinetics and particle growth.

As an example, for the synthesis of ~100 nm silica nanoparticles, a mixed solution containing ammonia (0.5 mol), water (10 mol), and anhydrous ethanol was preheated to the desired reaction temperature. Separately, a preheated mixture of TEOS (0.2 mol) in anhydrous ethanol was prepared. The TEOS mixture was then rapidly added to the ammonia–water–ethanol solution under vigorous magnetic stirring. Fast and uniform mixing at this stage is crucial—it ensures simultaneous nucleation of silica seeds throughout the reaction volume, leading to uniform particle size. Within approximately 5 minutes, the reaction mixture gradually changed from colorless to milky white, indicating the formation of silica nuclei. The more uniform these initial nano-seeds are, the more monodisperse the final nanoparticles will be. The reaction was allowed to proceed for 2 hours, enabling controlled growth of the silica spheres to the target size. Upon completion, the nanoparticle suspension was centrifuged and washed several times with ethanol and water to remove unreacted precursors and byproducts, yielding clean, monodisperse silica nanoparticles ready for photonic crystal assembly.

To confirm the morphology and size of the synthesized nanoparticles, we characterized them using transmission electron microscopy (TEM) and dynamic light scattering (DLS) (see Experimental Section for sample preparation details). The results are presented in Figures 4 and 5. TEM images revealed that the silica nanoparticles have an average diameter of 103 ± 5 nm, in close agreement with the target size. The measured polydispersity index (PDI) was less than 5%, indicating excellent size uniformity and monodispersity. DLS analysis further supported these findings. The size distribution curve for the 100 nm silica nanoparticles exhibited a unimodal peak without any secondary or satellite peaks, confirming the absence of significant aggregation or size heterogeneity. The hydrodynamic diameter measured by DLS was 174.18 nm, which is larger than the TEM-measured dry-state size. This difference arises because DLS measures the hydrodynamic size, which includes the particle's solvation layer and any surface-bound molecules in the liquid medium, whereas TEM measures the physical core diameter in the dry state.

The color generated by photonic crystals can be predicted using Bragg's law ($\lambda = 2nd$), where λ is the reflected wavelength, n is the effective refractive index of the system, and d is the interparticle spacing, which corresponds to the nanoparticle diameter in closely packed lattices. For a given material system, the composition and hence n remain essentially constant, so the reflected color is

DOI: 10.54254/2755-2721/2026.KA27726

primarily determined by particle size. Therefore, by tuning the nanoparticle diameter, the reflected structural color of the 3D photonic crystal can be systematically adjusted.

Once the methodology for synthesizing and characterizing monodisperse silica nanoparticles was established, it became straightforward to prepare particles of different sizes. In the Stöber synthesis, particle size can be controlled by adjusting the concentrations of ammonia (catalyst) and TEOS (precursor). At a fixed TEOS concentration, increasing the ammonia concentration reduces the number of nucleation sites while accelerating particle growth, leading to larger nanoparticles. In our system (see Experimental Section), starting from the optimized conditions for 100 nm particles, we increased the ammonia concentration by 2- and 4-fold to obtain nanoparticles of approximately 150 nm and 200 nm, respectively. TEM images (Figure 4) confirmed that these particles exhibited excellent size uniformity, perfect sphericity, and smooth, defect-free surfaces, demonstrating outstanding morphologies and monodispersity. Corresponding DLS measurements (Figure 5) gave hydrodynamic diameters of 174.18 nm and 210.99 nm, which followed the same trend but were slightly larger than the TEM-derived sizes (～160 nm and ～205 nm).

Similarly, when the ammonia concentration was fixed at 1 mol, increasing the TEOS concentration resulted in both larger nuclei at the early stage and faster growth due to higher precursor availability. This adjustment successfully produced nanoparticles with diameters of approximately 341.65 nm and 390.12 nm, again without compromising monodispersity (Figure 5). Notably, the DLS curves for all samples exhibited symmetric unimodal peaks with no secondary or aggregation peaks, confirming that the suspensions were stable and well-dispersed under measurement conditions. Together, these results demonstrate that the Stöber method is a highly refined and reliable approach for producing monodisperse silica nanoparticles across a wide size range. TEM provided direct evidence of particle morphology and uniformity, while DLS offered complementary size information in the liquid state. The excellent agreement between the two methods validates the reproducibility of the synthesis. Importantly, the ability to precisely tune nanoparticle size provides a robust foundation for fabricating high-quality photonic crystal films, enabling full-spectrum structural color tuning and potential temperature-responsive functionalities.

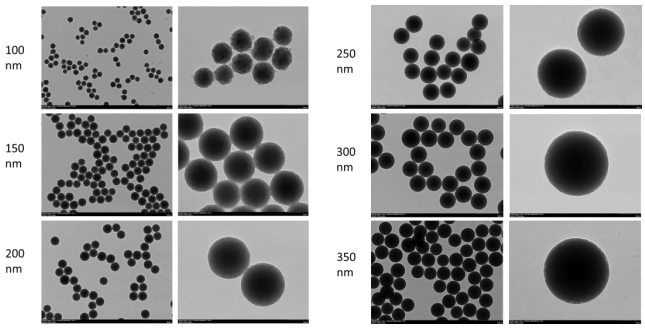

Figure 4. Transmission Electron Microscopy (TEM) images of monodisperse silica nanoparticles with diameters of 100, 150, 200, 250, 300, and 350 nm. All microspheres exhibit outstanding monodispersity

DOI: 10.54254/2755-2721/2026.KA27726

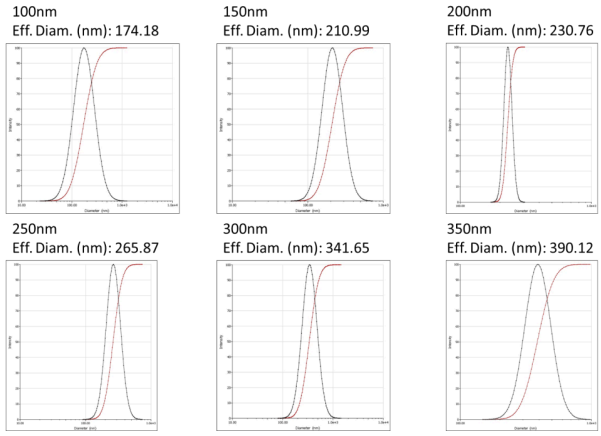

Figure 5. Dynamic Light Scattering (DLS) curves of silica nanoparticles with different diameters of 100, 150, 200, 250, 300, and 350 nm

3.2. Self-assembly of silica nanoparticles

As discussed in Section 3.1, while the uniformity of nanoparticles strongly influences the crystalline structure and, consequently, the quality of the resulting color, the self-assembly method employed is equally critical. Even when nanoparticles with the same low polydispersity are used, different assembly processes can yield crystalline structures of varying quality. To achieve precise control and minimize defects, we employed the vertical deposition self-assembly method for fabricating photonic crystal films.

As illustrated in Figure 3, this method involves slowly evaporating a suspension of monodisperse nanoparticles in a volatile solvent (typically water or ethanol) while a substrate is held vertically (or at a slight tilt) inside the suspension. During evaporation, capillary forces at the liquid–air–substrate interface drive the nanoparticles into close-packed arrangements. Once the first monolayer is pinned, subsequent particles deposit layer by layer, resulting in the growth of ordered multilayered crystalline structures. When evaporation occurs gradually and the nanoparticles are highly uniform, the process produces large-area films with minimized defects. With appropriately sized nanoparticles, these ordered 2D or 3D colloidal crystal films display intense, angle-dependent structural colors.

Among the various self-assembly strategies, the vertical deposition method offers several advantages: (1) Simplicity – requiring only basic equipment and straightforward operation. (2) Controllability – enabling precise control over crystal ordering and film thickness. (3) Scalability – allowing the fabrication of large-area films within practical timeframes. These advantages make vertical deposition a highly effective method for producing high-quality photonic crystals. Accordingly, it was selected in this study to prepare structurally colored photonic crystal films.

As described in the Experimental Section, glass substrates were first thoroughly cleaned by ultrasonic washing to remove any surface impurities, which could otherwise disrupt nanoparticle packing. The SiO_2 suspensions were also ultrasonicated for 1 hour to prevent aggregation or sedimentation, ensuring high-quality dispersions. The well-dispersed suspensions were poured into cylindrical glass vials, into which the cleaned glass slides were vertically inserted. The vials were then placed in a 60 °C constant-temperature incubator for 60 hours, allowing for the gradual vertical deposition and crystal growth.

The resulting films were characterized by scanning electron microscopy (SEM) Figure 6. The images clearly reveal that nanoparticles of varying sizes were successfully assembled into highly

DOI: 10.54254/2755-2721/2026.KA27726

ordered, continuous structures with excellent uniformity. The films exhibited intact crystalline domains without obvious voids or fabrication defects, confirming the efficiency of vertical deposition in generating high-quality crystal-like structures. To further verify the crystallinity, SEM images of films assembled from silica nanoparticles with diameters of 150, 250, and 350 nm were analyzed using the Fast Fourier Transform (FFT) method. As shown in Figure 7, the FFT patterns displayed distinct periodic diffraction spots rather than diffuse rings, confirming the presence of single-crystalline or highly ordered domains rather than polycrystalline or amorphous structures. Moreover, the diffraction spots exhibited clear sixfold symmetry, characteristic of a hexagonal close-packed (hcp) arrangement of the silica nanoparticles. Collectively, these results demonstrate that the vertical deposition method reliably produces well-ordered colloidal crystal films, establishing it as a robust platform for structural color generation.

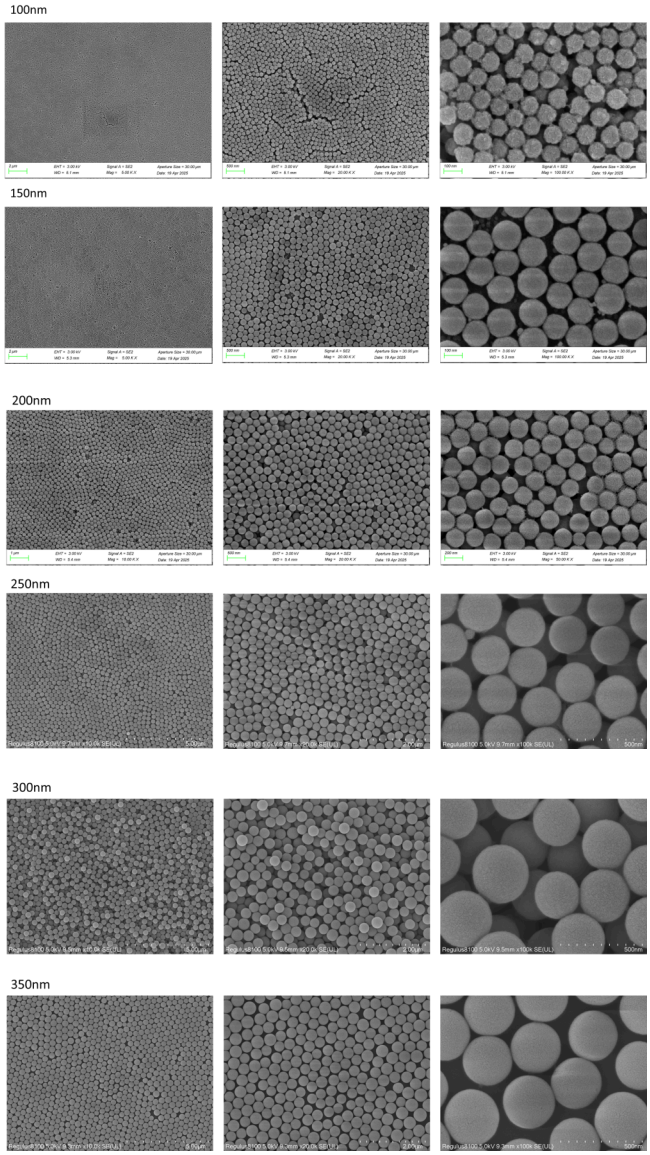

Figure 6. Scanning Electron Microscopy (SEM) images of self-assembled films deposited from silica nanoparticles with different diameters of 100, 150, 200, 250, 300, and 350 nm

DOI: 10.54254/2755-2721/2026.KA27726

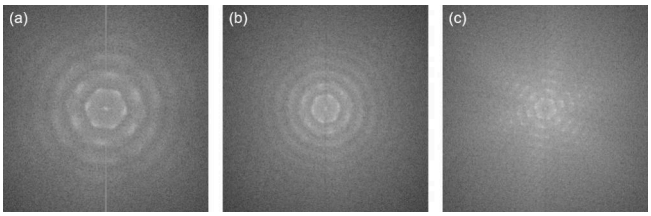

Figure 7. Fast Fourier Transform (FFT) images from the SEM images of self-assembled films deposited from silica nanoparticles with different diameters of 150 (a), 250 (b), and 350 nm (c)

3.3. Structural color of photonic crystals

Considering the well-ordered crystal-like structures observed in the SEM images, it is expected that these nanoparticle assemblies exhibit structural colors, behaving as photonic crystals. This expectation is confirmed by the photographs and optical microscope images of the films shown in Figures 8 and 9. For example, when the diameter of the silica nanoparticles targeted 200 nm (corresponding to a hydrodynamic diameter of ~231 nm from DLS), the resulting film displayed a bright blue color. Interestingly, a gradient in color variation was also observed across the film. The same gradient pattern was visible under an optical microscope even when the sample was placed flat, ruling out angular iridescence from sample tilting as the cause. Although further characterization and control experiments are needed to fully explain this effect, we hypothesize that it arises from variations in film thickness or the presence of localized defects during the vertical deposition process. These variations would result in spatially dependent reflection of different wavelengths, giving rise to color gradients.

As described in Section 3.1, the reflected color of photonic crystals is closely correlated with nanoparticle diameter in accordance with Bragg's law. This size–color relationship is clearly demonstrated in Figures 8 and 9. As the nanoparticle diameter increased from ~231 nm to 266 nm and 342 nm (corresponding to target sizes of 250 and 300 nm), the reflected color redshifted from blue to green and then to red, consistent with theoretical predictions. Further increasing the nanoparticle size to 390 nm produced a faint pink hue. This pink coloration can be understood as a superposition of red and second-order blue contributions, while the diminished intensity is attributed to the red component being shifted into the deep-red or near-infrared region, which contributes little to visible color perception.

Notably, in all samples a layered stripe-like color pattern was observed. This feature is partially attributed to defects inherent in the vertical deposition process, which disrupt uniform color reflection. In addition, the pattern may also originate from drying-induced cracks, a limitation that will be addressed in the following section through the incorporation of hydrogel. Furthermore, when the silica nanoparticle size was below ~231 nm (e.g., at 174 and 211 nm), the films exhibited rainbow-like colors without a consistent trend. This phenomenon is likely due to thin-film interference effects, similar to those seen in soap bubbles, rather than photonic bandgap reflection from a well-formed 3D crystal lattice. Together, these results confirm that the vertical deposition self-assembly of monodisperse silica nanoparticles yields structurally colored photonic crystal films whose color can be systematically tuned by particle size, while also revealing the influence of film thickness and assembly defects on optical performance.

DOI: 10.54254/2755-2721/2026.KA27726

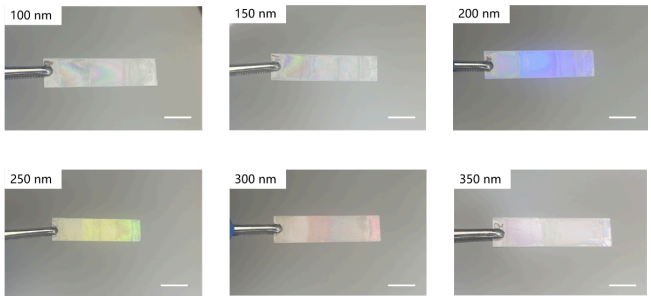

Figure 8. Photographs of photonic crystal structural color films fabricated from silica nanoparticles with diameters of 100, 150, 200, 250, 300, and 350 nm, taken with a camera and optical microscope. Scale bar: 1 cm

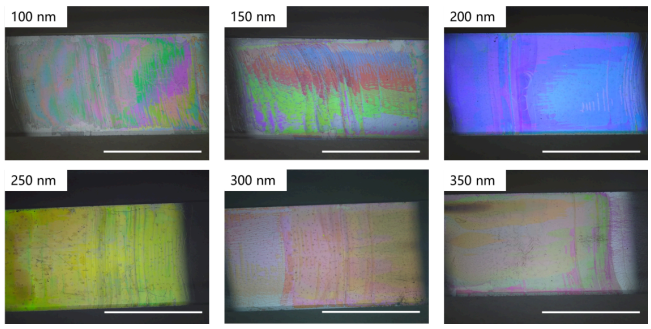

Figure 9. Optical microscopy images of photonic crystal structural color films fabricated from silica particles with diameters of 100, 150, 200, 250, 300, and 350 nm. Scale bar: 1 cm

3.4. Fabrication and thermo-responsive behavior of photonic hydrogel

As mentioned in Section 3.3, the self-assembled films of silica nanoparticles suffered from cracking and fragility, since aggregates of nanoparticles are mechanically weak and prone to fracture. This limitation significantly restricts the practical applications of photonic crystal films. To overcome this problem, we propose a photonic hydrogel (i.e., hydrogel–photonic crystal composite) system. In this design, the hydrogel acts as a polymer crosslinking scaffold that firmly embeds and stabilizes the self-assembled photonic crystal structures, thereby maintaining their integrity even under mechanical stress. Beyond structural reinforcement, the hydrogel composition can be tailored to impart stimuli-responsive properties. For instance, a thermo-responsive hydrogel enables tuning of the interparticle spacing in response to temperature changes, leading to dynamic color modulation of the photonic crystal film. Such thermo-responsive composites hold great promise for applications in temperature indicators, decorative coatings, and radiative cooling materials.

However, fabricating these composites is not as straightforward as simply mixing the components. The pre-assembled photonic crystal order must be preserved during infiltration of the hydrogel precursor solution and subsequent polymerization. As described in the experimental section, the aqueous precursor solution was formulated with acrylamide and acrylic acid as monomers), N,N′-methylenebisacrylamide as the crosslinker, and photoinitiator. The precursor solution was carefully introduced onto the preformed photonic crystal arrays to minimize disruption of nanoparticle order. Polymerization was then carried out under ultraviolet (UV) light at low temperature, a critical condition that reduces fluid convection and thereby helps preserve the crystal-like arrangement of nanoparticles.

DOI: 10.54254/2755-2721/2026.KA27726

After polymerization, the resulting hydrogel–photonic crystal composite was gently peeled off and transferred to water to yield a free-standing, temperature-responsive film. As shown in Figure 10, we successfully fabricated a palm-sized composite with bright green and red structural colors under swollen conditions. These observations confirm that the ordered photonic crystal lattice was preserved throughout precursor diffusion and hydrogel crosslinking. Moreover, the hydrogel matrix imparted excellent structural integrity, enabling the film to remain intact as a free-standing sheet in aqueous media. Although some non-uniformity in color existed, the optical quality was sufficient to serve as a strong proof-of-concept demonstration of a large-area hydrogel–photonic crystal composite.

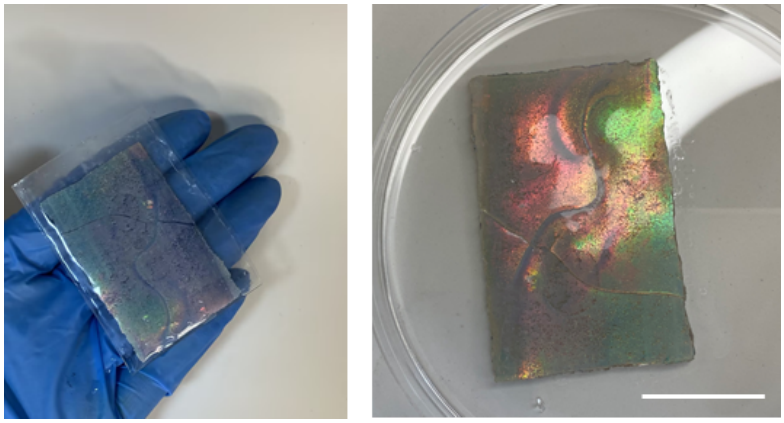

Figure 10. Optical images of the hydrogel-photonic crystal composite

To evaluate its thermo-responsive behavior, the composite was subjected to controlled heating. As shown in Figure 11, when the temperature increased from 26 °C to 36 °C, the hydrogel contracted due to the temperature-dependent hydrophobicity of polyacrylamide, which expels water at elevated temperatures. This contraction reduced the lattice spacing of the embedded photonic crystal, producing a visible color shift from red to blue.

The thermo-optical response was quantified using in situ temperature-dependent UV–vis spectroscopy Figure 12. In the first heating cycle, the reflection peak wavelength shifted from 590 nm at 27 °C to 545 nm at 31 °C, and further to 500 nm at 33 °C, clearly demonstrating a blueshift. Upon cooling and repeating the measurements, the shift was fully reversible, and nearly identical behavior was observed in the second cycle, confirming the robustness and repeatability of the hydrogel–photonic crystal composite. Mechanistically, the hydrogel is initially swollen in water, yielding a larger lattice spacing and diffraction at longer wavelengths. Upon heating, the hydrogel contracts, reducing the interparticle distance and shifting the photonic bandgap toward shorter wavelengths, a phenomenon well-known as blue-shifting in responsive photonic systems.

DOI: 10.54254/2755-2721/2026.KA27726

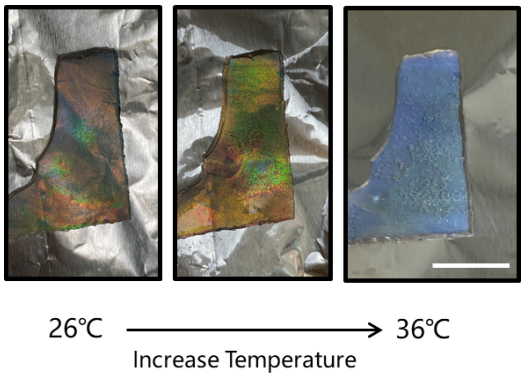

Figure 11. Optical photographs of the hydrogel film at increasing temperatures. Scale bar: 1 cm

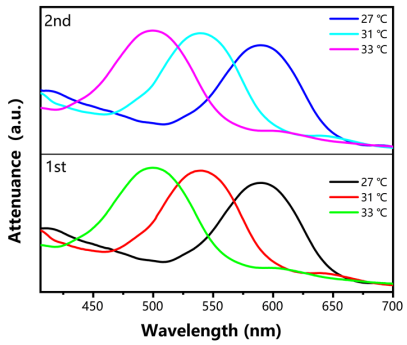

Figure 12. In situ temperature-dependent UV–vis spectra of photonic crystal hydrogels at different temperatures. Spectra at 27 °C, 31 °C, and 33 °C are used as references, showing the temperature-dependent blue shift of the diffraction wavelength

3.5. Further investigation into temperature indicator and radiative cooling

The previous sections have demonstrated that large-area hydrogel–photonic crystal composites can be successfully fabricated with bright and tunable structural colors. These colors can be controlled intrinsically by the diameter of silica nanoparticles, which dictates the photonic bandgap, and dynamically modulated through the thermo-responsive swelling and contraction of the hydrogel matrix. Together, these features position the material as a versatile platform with broad potential in functional coatings, optical sensors, and energy-efficient building materials. Representative application scenarios, including temperature indicators, decorative coatings, and radiative cooling devices, are illustrated in Figure 13.

As a proof-of-concept, we will demonstrate the integration of these composites into smart window systems, where the photonic film is encapsulated between two glass layers. By patterning the hydrogel–photonic crystal into distinct shapes or characters, one can realize temperature-responsive optical displays, such as the demonstration shown in Figure 13: “>32 °C We are getting warm here.” In this design, the glass appears light red at T < 26 °C, reflecting longer wavelengths of visible light (620–750 nm). As the temperature rises beyond 32 °C, the hydrogel contracts, reducing lattice spacing and inducing a blue-shift in the reflected color to the shorter wavelength region (380–500 nm). This visible transition enables the glass to function as both a real-time temperature indicator and a decorative element with dynamic optical properties.

DOI: 10.54254/2755-2721/2026.KA27726

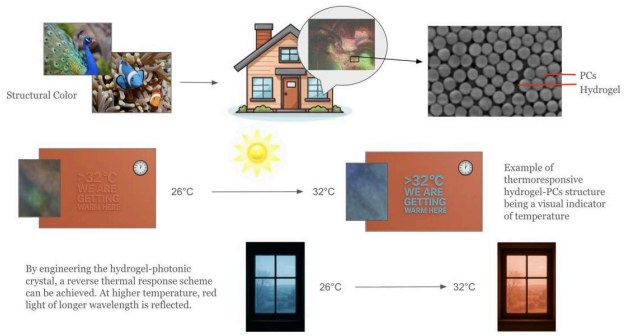

Figure 13. Schematic illustration of the current hydrogel–photonic crystal system and two potential application scenarios: (i) temperature indication and (ii) radiative cooling

Notably, the thermo-responsive behavior can be further engineered. While the current system relies on hydrogel contraction at elevated temperatures (thermo-contraction), alternative materials with thermo-expansion behavior could be employed to achieve the reverse color scheme (from blue to red upon heating). Such a configuration may be more intuitive for users, since red is instinctively associated with warmth and danger in human perception, while blue conveys coolness. This design consideration illustrates how materials science and human-factor engineering can be combined to optimize functional coatings for real-world applications.

Beyond sensing and decoration, the hydrogel–photonic crystal composites also hold promise for radiative cooling, a passive thermal management strategy that relies on selective reflection and emission of infrared radiation. When embedded in glass window structures, the composite can contribute through three distinct mechanisms:

(1) Passive cooling by the hydrogel matrix: Hydrogels are predominantly water-based and exhibit strong vibrational modes in the infrared region, granting them naturally high IR emissivity. This property allows them to effectively radiate thermal energy away from the building, thereby reducing internal heat buildup.

(2) Broadening of thermal emission by silica nanoparticles: The silica nanoparticles not only form the photonic lattice but also exhibit surface phonon resonances, particularly in the 8–13 μm range of the atmospheric transparency window. Thus, incorporating silica enhances cooling performance by expanding emissivity in this crucial spectral region.

(3) Targeted solar reflection by photonic crystals: By tuning nanoparticle size and lattice periodicity, the photonic crystal can be designed to selectively reflect portions of the solar spectrum. Reflecting light in the deep red/near-infrared region (600 nm–2.5 μm), which constitutes more than 50% of the solar energy flux, is particularly beneficial because it reduces solar heat.

Our results represent an initial but significant step toward radiative cooling windows. The fabricated composites exhibited reversible color shifts under thermal cycling, demonstrating the potential for dynamic solar management. With further optimization, such materials could be engineered to reflect infrared radiation at elevated temperatures ($T > 32$ °C), thereby decreasing unwanted heat input, while still exhibiting visible structural colors that provide both aesthetic value and functional temperature feedback. At lower temperatures ($T < 26$ °C), the glass could instead permit controlled transmission of red/NIR light to improve thermal comfort indoors during cooler conditions.

In addition to their physical effects on energy transfer, these color changes have a psychological dimension. According to the Hue–Heat hypothesis [23], people perceive cooler-colored

DOI: 10.54254/2755-2721/2026.KA27726

environments (e.g., blue tones) as colder than warmer-colored environments (e.g., red tones), even when the actual temperature remains unchanged. This suggests that the hydrogel–photonic crystal glass can reduce the perceived need for air conditioning through visual cues, complementing its passive radiative cooling function. Such a dual mechanism, physical energy management and psychological thermal modulation, offers a uniquely sustainable approach to reducing energy consumption in buildings. This also provide a large space for the future design and achievement in the application of this hydrogel–photonic crystal glass in the building materials as demanded.

4. Conclusion

In this study, we have demonstrated a complete workflow for designing, synthesizing, and utilizing monodisperse silica nanoparticles to fabricate structurally colored photonic crystal films and their hydrogel-based composites with tunable optical properties. The Stöber method enabled the controlled synthesis of silica nanoparticles with excellent monodispersity and size uniformity, which is critical for achieving high-quality 3D photonic crystal structures. Nanoparticle size was shown to directly influence the reflected structural color, in excellent agreement with Bragg's law, allowing systematic color tuning across the visible spectrum.

Using the vertical deposition self-assembly method, we successfully constructed large-area, defect-minimized photonic crystal films. SEM and FFT analysis confirmed highly ordered hexagonal close-packed arrangements, while optical characterization demonstrated vivid structural colors. The results also highlighted the effects of film thickness, assembly defects, and nanoparticle size on optical performance, emphasizing the importance of careful control over self-assembly conditions.

To address mechanical fragility and cracking in the free-standing photonic crystal films, we developed hydrogel–photonic crystal composites. The hydrogel scaffold maintained structural integrity while preserving the ordered nanoparticle arrangement, enabling free-standing, large-area films that could sustain swelling and handling without structural failure. Importantly, the hydrogel endowed the composites with thermo-responsive properties, producing reversible color shifts in response to temperature changes. In situ UV–vis measurements confirmed reliable and repeatable blue-shifts with increasing temperature, demonstrating robust dynamic optical behavior.

Finally, we outlooked to explore potential practical applications of these composites in the future. As a temperature indicator, the films can be patterned within smart windows to provide visual cues about ambient conditions, with possibilities for customized color–temperature responses. As a radiative cooling material, the system can leverage the IR emissivity of the hydrogel, thermal emission broadening by silica nanoparticles, and targeted reflection by photonic crystals to passively manage solar heat input while maintaining aesthetic appeal. The combination of physical thermal regulation and psychological perception of color offers a dual mechanism for energy-efficient building design.

Overall, this work demonstrates a versatile, scalable platform for tunable photonic crystals and stimuli-responsive composites, providing both fundamental insight into nanoparticle self-assembly and practical strategies for functional optical materials. The study establishes a foundation for future exploration of large-scale, durable, and responsive photonic devices, with promising applications in sensing, decoration, and energy-efficient smart materials.

DOI: 10.54254/2755-2721/2026.KA27726

References

[1] Ritchie, H. (2024). Air Conditioning Causes around 3% of Greenhouse Gas Emissions. How Will This Change in the Future? Our World in Data.

[2] Shang, J.; Zhang, Y.; Zhang, J.; Zhang, X.; An, Q. (2024). Hydrogel-Based Stimuli-Responsive Radiative and/or Evaporative Cooling Materials for Carbon Neutrality. ACS Energy Letters 9, 594-626.

[3] Wang, T.; Zhang, S.; Zhu, Q.; Zhang, J.; Zhang, Y.; Du, Y.; Wu, L.; Gu, M.; Zhang, Y. (2024). A Trilayer Structure with Surface Binary Microsphere Array for Radiative Cooling and Heating Regulation. ACS Photonics, 11, 2815-2823.

[4] Zhao, J.; Nan, F.; Zhou, L.; Huang, H.; Zhou, G.; Zhu, Y.-f.; Ou, Q. (2023). Free-Standing, Colored, Polymer Film with Composite Opal Photonic Crystal Structure for Efficient Passive Daytime Radiative Cooling. Solar Energy Materials and Solar Cells, 251, 112136.

[5] Huang, G.; Yengannagari, A. R.; Matsumori, K.; Patel, P.; Datla, A.; Trindade, K.; Amarsanaa, E.; Zhao, T.; Köhler, U.; Busko, D.; Richards, B. S. (2024). Radiative Cooling and Indoor Light Management Enabled by a Transparent and Self-Cleaning Polymer-Based Metamaterial. Nature Communications, 15, 3798.

[6] Huang, L.; Hu, Y.; Yao, X.; Chesman, A. S. R.; Wang, H.; Sagoe-Crentsil, K.; Duan, W. (2024). Designing Nanoporous Polymer Films for High-Performance Passive Daytime Radiative Cooling. ACS Applied Materials & Interfaces, 16, 54401-54411.

[7] Yue, Y.; Gong, J. P. (2015). Tunable One-Dimensional Photonic Crystals from Soft Materials. Journal of Photochemistry and Photobiology C: Photochemistry Reviews, 23, 45-67.

[8] Kim, S.-H.; Lee, S. Y.; Yang, S.-M.; Yi, G.-R. (2011). Self-Assembled Colloidal Structures for Photonics. NPG Asia Materials, 3, 25-33.

[9] Cai, Z.; Li, Z.; Ravaine, S.; He, M.; Song, Y.; Yin, Y.; Zheng, H.; Teng, J.; Zhang, A. (2021). From Colloidal Particles to Photonic Crystals: Advances in Self-Assembly and Their Emerging Applications. Chemical Society Reviews, 50, 5898-5951.

[10] Zhao, Y.; Shang, L.; Cheng, Y.; Gu, Z. (2014). Spherical Colloidal Photonic Crystals. Accounts of Chemical Research, 47, 3632-3642.

[11] Goyal, A. K. (2024). Introductory Chapter: Photonic Crystal Technology – Introduction, Advantage, and Applications. In Recent Advances and Trends in Photonic Crystal Technology, Goyal, A. K.; Kumar, A., Eds. IntechOpen: Rijeka.

[12] Laftah, W. A.; Hashim, S.; Ibrahim, A. N. (2011). Polymer Hydrogels: A Review. Polymer-Plastics Technology and Engineering, 50, 1475-1486.

[13] Kim, Y.-J.; Matsunaga, Y. T. Thermo-Responsive Polymers and Their Application as Smart Biomaterials. Journal of Materials Chemistry B 2017, 5, 4307-4321.

[14] Dai, S.; Ravi, P.; Tam, K. C. (2009). Thermo- and Photo-Responsive Polymeric Systems. Soft Matter, 5, 2513-2533.

[15] Tian, J.; Peng, H.; Du, X.; Wang, H.; Cheng, X.; Du, Z. (2021). Hybrid Thermochromic Microgels Based on Ucnps/Pnipam Hydrogel for Smart Window with Enhanced Solar Modulation. Journal of Alloys and Compounds, 858, 157725.

[16] Zhou, Y.; Cai, Y.; Hu, X.; Long, Y. (2014). Temperature-Responsive Hydrogel with Ultra-Large Solar Modulation and High Luminous Transmission for “Smart Window” Applications. Journal of Materials Chemistry A, 2, 13550-13555.

[17] Guo, R.; Shen, Y.; Chen, Y.; Cheng, C.; Ye, C.; Tang, S. (2024). Kca/Na2sio3/Pnipam Hydrogel with Highly Robust and Strong Solar Modulation Capability for Thermochromic Smart Window. Chemical Engineering Journal, 486, 150194.

[18] Fang, Z.; Ding, L.; Li, L.; Shuai, K.; Cao, B.; Zhong, Y.; Meng, Z.; Xia, Z. (2021). Thermal Homeostasis Enabled by Dynamically Regulating the Passive Radiative Cooling and Solar Heating Based on a Thermochromic Hydrogel. ACS Photonics, 8, 2781-2790.

[19] Lee, M.; Kim, G.; Jung, Y.; Pyun, K. R.; Lee, J.; Kim, B.-W.; Ko, S. H. (2023). Photonic Structures in Radiative Cooling. Light: Science & Applications, 12, 134.

[20] Nan, F.; Zhu, Y.-F.; Wei, H.-X.; Lin, Y.; Fan, B.; Zhou, L. (2022). Flexible Composite Film with Artificial Opal Photonic Crystals for Efficient All-Day Passive Radiative Cooling. Optics Express, 30, 6003-6015.

[21] Shang, J.; Zhang, J.; Zhang, Y.; Zhang, X.; An, Q. (2024). Highly Potent Transparent Passive Cooling Coating Via Microphase-Separated Hydrogel Combining Radiative and Evaporative Cooling. Nano Letters, 24, 7055-7062.

[22] Miller, B. H.; Liu, H.; Kolle, M. (2022). Scalable Optical Manufacture of Dynamic Structural Colour in Stretchable Materials. Nature Materials, 21, 1014-1018.

DOI: 10.54254/2755-2721/2026.KA27726

[23] Hammond, B. R.; Gardner, C. R.; Wooten, B. R.; Renzi-Hammond, L. (2024). Increasing Intensity Directly Increases the Perceived Warmth of Primary Colors. Scientific Reports, 14, 26852.